

STRUCTURE DESIGN AND MECHANICAL SIMULATION ON THE SC-MR SUPPORT FOR ROTOR SYSTEM

Yanhong Ma, Haixiong Zhu, Jie Hong
School of Energy and Power Engineering, BUAA

Keywords: *SC-MR support, Loading position, Pre-compression*

Abstract

A typical elastic damping support combined of squirrel cage and metal rubber is proposed here and named SC-MR support for short. This paper mainly deals with the structure design of the SC-MR support and the numerical simulation on its support stiffness. The technical approach on its structure design was given and the simulation models were established. Both the radial stiffness and the angular stiffness were researched by simulation, and the impacts of the loading position as well as the assembling state were obtained. The simulation results show that the loading position has a great effect on the support stiffness of the squirrel cage and the SC-MR support, especially the angular stiffness. While the loading position moved from the left ring to the right one, the radial stiffness varied by 25% and the angular stiffness varied by as much as 80%. The results also imply that both the radial stiffness and angular stiffness exhibit nonlinear increasing trends with the increase of the radial pre-compression. While the radial prestrain increased from 0.6% to 3.16%, the radial stiffness increased by 17.3% and the angular stiffness increased by 51.6%. The angular stiffness appeared to be more sensitive to either the loading position or the assembling state.

1 Introduction

In high speed rotating machineries such as small sized gas turbine engines and turbo booster pumps, the rotor system is usually designed to be flexible and the working speed is usually above several critical speeds as discussed in [1]. For such machineries, the vibration control is a

great challenge to the security and performance of the system. As a consequence of the high speed, the exciting force caused by the imbalance could reach a considerable level. While traversing the critical speed during the speed up/down process, the rotor system may suffer from a severe vibration.

The combination of the elastic support and damper provides a wonderful solution to the vibration problems, with the flexible support adjusting the critical speeds and the damper dissipating the vibration energy. In aeroengines, the squirrel cages or elastic rings working with SFD are usually designed at the bearing casing. This structure is widely used due to its simple construction, low cost and remarkable performance at certain ranges. But the shortcomings are obvious. Whenever the exciting force caused by the imbalance become much larger than the designed value, the bearing stiffness of the oil film would increase strongly nonlinearly with the increase of the eccentricity ratio and the rotor system may suffer from the bistable state, the nonsynchronous whirls and the instability due to the strong nonlinear characteristics, as reported in [2,3]. What's more, the design of the oil supply system may be complex and even unrealizable at some severe conditions.

In recent researches, the elastic damping support was improved and novel styles were proposed such as the adaptive squeeze film damper with the metal rubber [4], the elastic ring-metal rubber support [5] and the metal mesh-gas foil bearing [6]. In these researches a novel damping material, the metal rubber (named MR for short), was used. MR is a promising damping material free of oil. It's a form of a tangled metallic mesh manufactured via a process of wire-drawing, weaving and compression

molding [7]. The term “metal rubber” arises from the similarity between the properties of MR and those of elastomeric rubber, although some authors do prefer to use the term of “metal mesh”, “entangled metallic wire material (EMWM)” or “wire mesh” to define this type of porous material [8]. As reported in [9,10], the metal rubber is easy to be fabricated into special shapes and can be used to almost all the working conditions in engines or pumps.

The elastic damping structure with MR has shown superior damping capacity, and showed promising prospects in engineering applications. The SC-MR support is such a typical structure, with the squirrel cage supplying the main support stiffness and the metal rubber supplying the main damping and parallel stiffness. Due to the structural characteristics of the SC-MR support, the mechanical properties can be designed to certain ranges. As [11] reported, the MR dampers in parallel with a squirrel cage allow wider control of the support stiffness. And due to researches on the mechanical properties of the MR [12,13,14], the modulus and the damping of the MR components are greatly affected by the density, dimension, wire material, dynamic force amplitude, preloads, installation, etc. As a result, the modulus and damping of MR components could be designed by adjusting the material parameters or applying preloads.

The MR used as bearing damper in a turboprop rotor has been researched in rotordynamic tests [15,16]. Results indicated promising characteristics of the MR from the damping and stiffness point of view. The performance of MR rings as bearing dampers at cryogenic temperatures was also investigated by [17,18]. In following researches in [19], the effects of installation and operational factors on the wire mesh bearing damper were researched. It was reported that the stiffness and damping of the wire mesh damper both increased with the axial compression and the radial interference. But for the MR damper in parallel with a squirrel cage (the SC-MR support in this paper), the effects of the loading position and the radial pre-compression on the overall stiffness were not widely researched by simulation.

For the rotor system with a SC-MR support, the support stiffness is usually the key factor to

be designed. As the SC-MR support is installed with two parallel bearings, the bending of the rotor is affected by the angular resistance of the support. In other words, the angular stiffness of the support could affect the dynamic characteristics of the rotor system as well as the radial stiffness. Researches on the angular stiffness of similar structures in rotor systems could be found in [20,21]. But for the SC-MR support, the research on the angular stiffness has not been widely reported yet, although it's of great importance.

The work in this paper mainly focused on the simulation of the SC-MR support. Both the radial stiffness and the angular stiffness were researched. The effects of the loading position and the pre-compression on the stiffness were simulated. The results could provide reference for the structure design of such rotor supports.

2 Design on structural and mechanical characteristics

The SC-MR support proposed in this paper is combined of the squirrel cage, the limit baffle, the end cover and the metal rubber ring. Fig.1 illustrates the main components comprising the SC-MR support and the detailed structure.

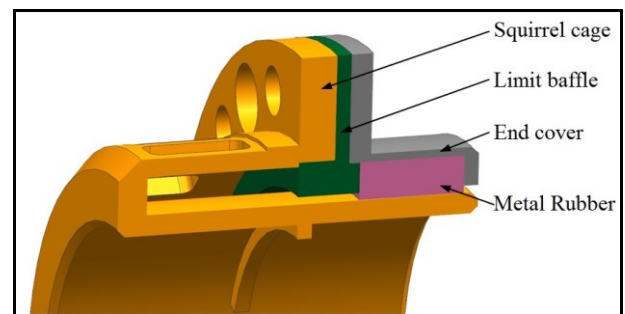


Fig.1 Structure of SC-MR support

As shown in Fig.1, the flanges of the squirrel cage, the limit baffle and the end cover are installed to the bearing casing together and the bearings are installed to the inner ring of the squirrel cage. The metal rubber ring is installed in the space surrounded by the limit baffle, the end cover and the inner ring of the squirrel cage. In SC-MR support, the main stiffness is supplied by the squirrel cage. When the radial force of the bearing is loaded, the squirrel cage deforms and the major part of the force is con-

ducted to the bearing casing. At the same time, the metal rubber ring is squeezed and the vibration energy is dissipated through the dry friction. On the other hand, the metal rubber ring transmits minor part of the force. Therefore, the metal rubber ring supplies the main damping and parallel stiffness to the squirrel cage.

During the design process, the main parameter to be controlled is the support stiffness. By adjusting the thickness, the length of the squirrel cage and the number of the bars, the main stiffness of the support could be set to a certain range. And by designing the parameters of the MR, such as the relative density, the parallel support stiffness could be set. The overall support stiffness could be adjusted by changing the preload of the MR.

3 The simulation method

3.1 FEM models

The FEM model of the squirrel cage is illustrated in Fig.2. Two rigid rings were built as the bearings, which contacted with the squirrel cage by contact pairs. The flange of the squirrel cage was fully constrained and the radial force was loaded on the rigid rings, similar to the real installation. The model was meshed with solid 185 elements and the material model of the squirrel cage was defined as 1045 steel ($E_s=210\text{GPa}$, $\rho_s=7.85\times 10^3\text{Kg/m}^3$, $\nu_s=0.3$). The friction coefficient μ_s of the contact was defined as 0.15.

Based on this model, the simulation under different loads could be realized. Under different working conditions, the loads of the bearings are different according to their deflections. The extreme condition comes into being when all the radial force is loaded on one bearing ring, either the left one or the right one. As a result, two extreme conditions exist and they compose the ultimate range of the loading position. During the simulation, three loading positions were simulated by applying the radial force on the left ring, on the right ring and on both two rings.

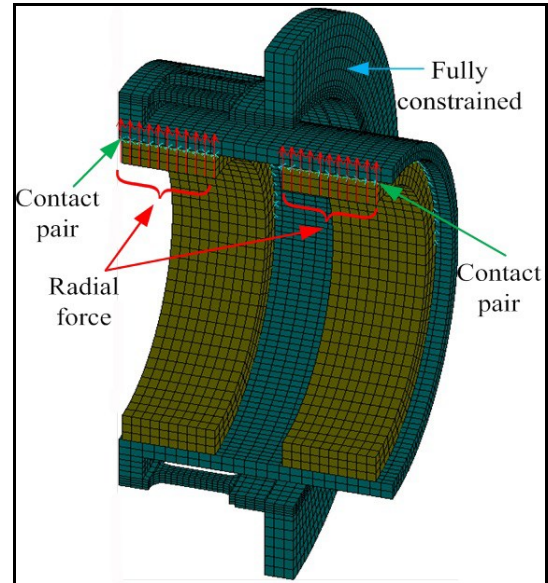


Fig.2 Model of the squirrel cage

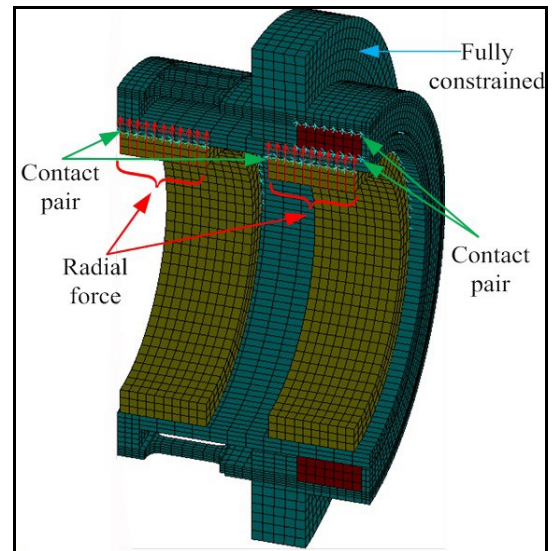


Fig.3 Model of the SC-MR support

The FEM model of the SC-MR support was built based on the model of the squirrel cage, as shown in Fig.3. The limit baffle and the end cover were added to the squirrel cage, and the metal rubber ring was built in the space surrounded by them. The metal rubber was also meshed with solid 185 elements and the material model was defined as MR. Contact pairs were built between the contact surfaces and the target surfaces as illustrated. The boundary conditions and the loads were the same as the model of the squirrel cage. In the same way, the simulation under different loads could be conducted.

3.2 Material model of the Metal Rubber

According to the nonlinear mechanical characteristics of the Metal Rubber, the Mooney-Rivlin model (a superelastic material model) was selected as the MR model. The parameters were extracted from the test data. The nonlinearity of the MR model was taken into account by applying the nonlinear stress-strain relationship to the model. In this way, the Young's modulus of the MR could be updated during the calculation. The nonlinear stress-strain relationship is shown by the curve before translation in Fig.4. Furthermore, to research the effect of the pre-compression, the nonlinear stress-strain curve was processed by a translation as shown in Fig.4.

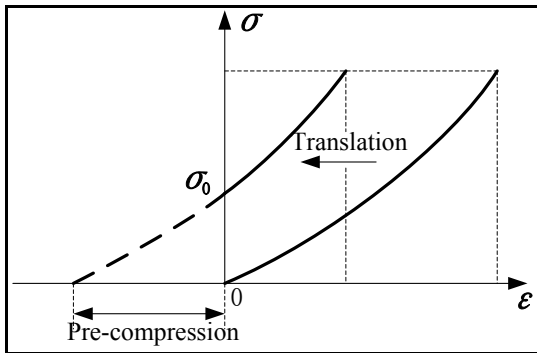


Fig.4 Equivalent stress-strain curve of metal rubber considering pre-compression

3.3 Method of the mechanical parameter prediction

During the simulation, the stiffness of the structure was calculated by the displacement of the rigid ring. As the radial force F is applied on the rigid ring, the structure deforms and the displacement of the rigid ring is shown in Fig.5.

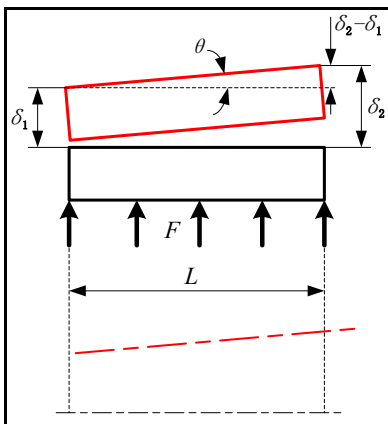


Fig.5 Displacement of the rigid ring

The radial displacements of two points were picked up as δ_1 and δ_2 , as illustrated in Fig.5. The average value of δ_1 and δ_2 was set to be the equivalent radial displacement of the structure, and the angular displacement θ was calculated, as illustrated in Eq.(1).

$$\begin{aligned} \delta &= (\delta_1 + \delta_2)/2 \\ \theta &= \arcsin[(\delta_2 - \delta_1)/L] \end{aligned} \quad (1)$$

The resultant force and bending moment was calculated by Eq.(2).

$$\begin{aligned} F &= n \cdot f \\ M &= \sum_{i=1}^n (f \cdot x_i) \end{aligned} \quad (2)$$

In the above equation, f is the component force applied on each node, n is the total number of the loaded nodes, x_i is the distance between the i^{th} node and the left end of the squirrel cage.

The support stiffness of the structure includes two parts, the radial stiffness and the angular stiffness. The radial one represents the resistance to the force in radial direction, and the angular one represents the resistance to the moment in angular direction. The radial stiffness and the angular stiffness could be calculated by Eq.(3).

$$\begin{aligned} K_r &= F/\delta \\ K_\theta &= M/\theta \end{aligned} \quad (3)$$

4 Result and discussion

4.1 The effect of the loading position

The deformation distribution of the squirrel cage with different loading positions is shown in Fig.6.

As shown by the deformation distribution, when the loading position was closer to the right side, the angular displacement of the bearing ring tended to be larger. The radial displacements of the reference points were extracted and the stiffness of the squirrel cage was obtained, as listed in Table 1.

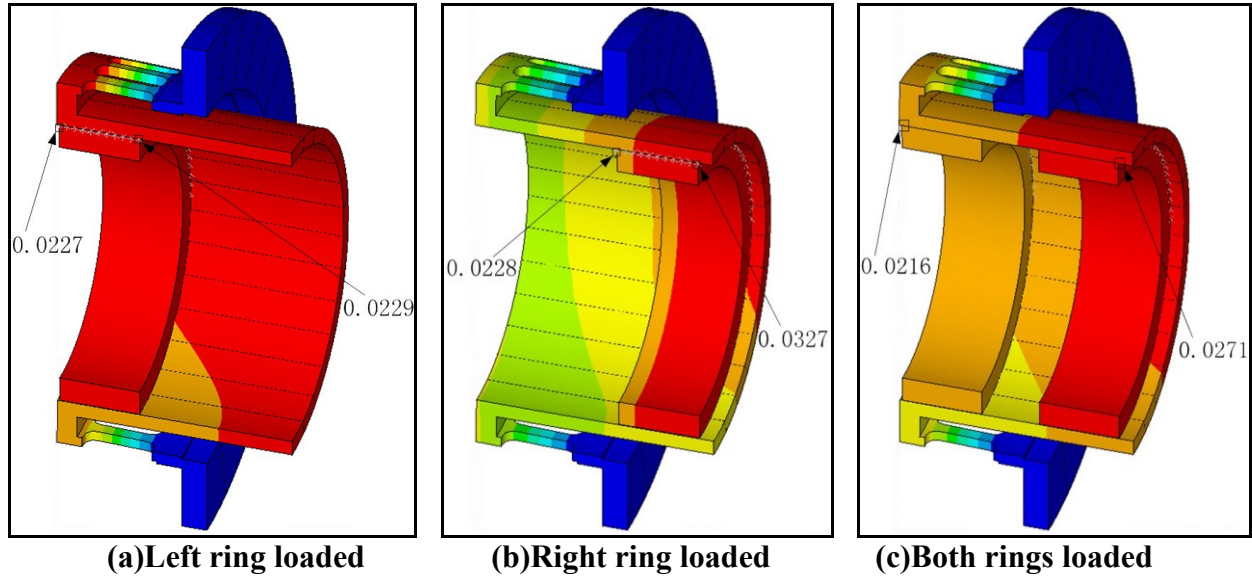


Fig.6 Deformation distribution of the Squirrel Cage

Table 1 Stiffness of the squirrel cage with different rings loaded

Model	δ_1 ($10^{-2}mm$)	δ_2 ($10^{-2}mm$)	δ ($10^{-2}mm$)	K_r ($10^7N/m$)	θ ($10^{-4}rad$)	K_θ ($10^5N\cdot m/rad$)
Left ring loaded	2.27	2.29	2.28	4.83	0.15	6.39
Right ring loaded	2.88	3.27	3.08	3.58	2.45	1.62
Both rings loaded	2.16	2.71	2.43	4.52	1.26	1.95

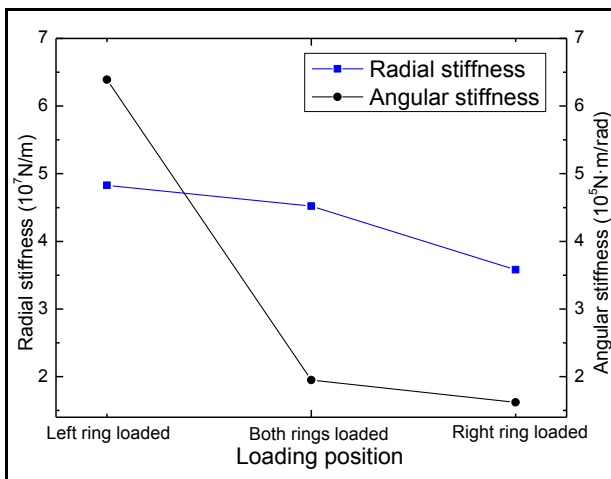


Fig.7 Stiffness of the Squirrel Cage vs. loading position

While the loading position was different, the varying trend of the radial stiffness and an-

gular stiffness of the squirrel cage are shown in Fig.7. As the loading position moves from the left ring to the right one, both the radial stiffness and the angular stiffness decreased. The radial stiffness decreased by 25.9%, while the angular stiffness decreased by 74.8%. It's obvious that the varying amplitude of the angular stiffness is much larger than that of the radial one. When the force was uniformly applied on the two rings, both the radial and angular stiffness were at an average value.

The similar deformation distribution of the SC-MR support with different loading positions is shown in Fig.8. The radial displacements of the reference points were extracted and the stiffness was listed in Table 2.

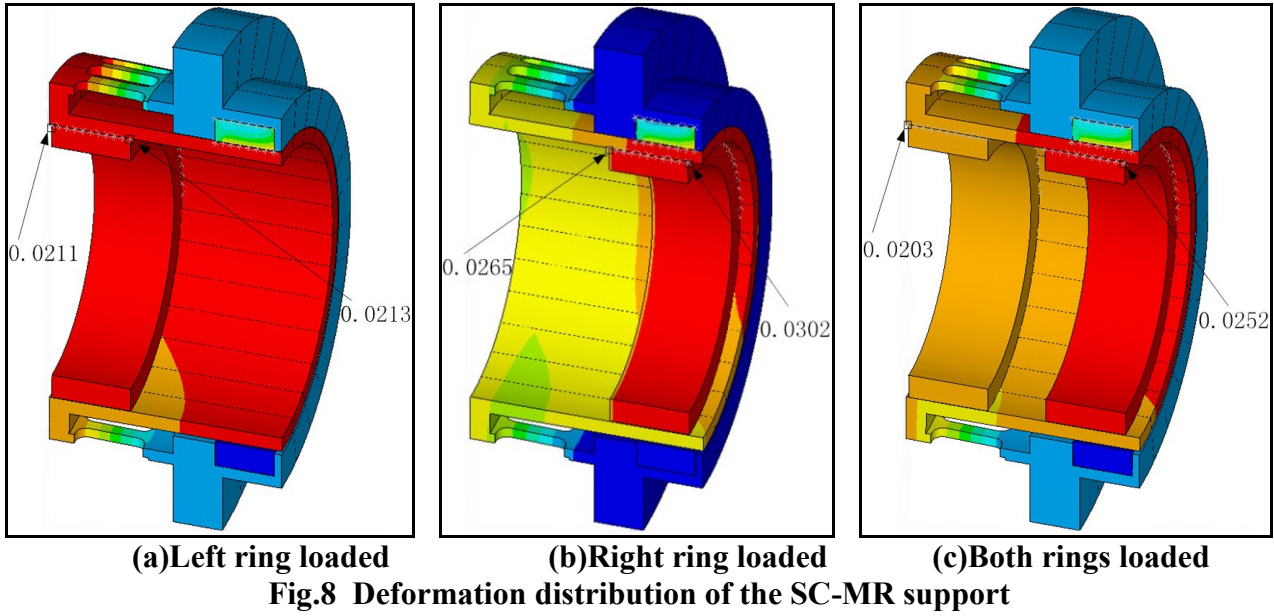


Table 2 Stiffness of the SC-MR support with different rings loaded

<i>Model</i>	δ_1 ($10^{-2}mm$)	δ_2 ($10^{-2}mm$)	δ ($10^{-2}mm$)	K_r ($10^7N/m$)	θ ($10^{-4}rad$)	K_θ ($10^5N\cdot m/rad$)
Left ring loaded	2.11	2.13	2.12	5.19	0.10	9.65
Right ring loaded	2.65	3.02	2.83	3.88	2.30	1.73
Both rings loaded	2.03	2.52	2.28	4.82	1.16	2.11

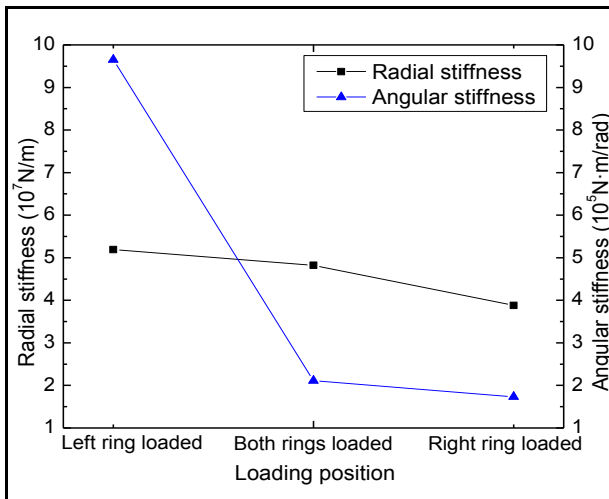


Fig.9 Stiffness of the SC-MR support vs. loading position

While the loading position was different, the varying trend of the radial stiffness and angular stiffness of the SC-MR support are shown in Fig.9. The data curves illustrated the similar varying trend as that of the squirrel cage. When

the loading position moved from the left ring to the right ring, the radial stiffness decreased by 25.2%; while the angular stiffness decreased by 82%. Compared to the result of the squirrel cage, the varying amplitude of the radial stiffness was nearly the same, but that of the angular stiffness became larger. It implies that the installation of the Metal Rubber contributed to the larger varying range of the angular stiffness.

4.2 The effect of the pre-compression

While the pre-compression of the Metal Rubber was different, the simulation was conducted by the same model but with different stress-strain relationships of the MR. The deformation distribution of the model was nearly the same as Fig.8(c), and the extracted radial displacements and the calculated stiffness are listed in Table 3.

Table 3 Stiffness of the support stiffness under different pre-strains

Radial pre-strain (%)	δ_1 (10^{-2} mm)	δ_2 (10^{-2} mm)	δ (10^{-2} mm)	K_r (10^7 N/m)	θ (10^{-4} rad)	K_θ (10^5 N·m/rad)
0.6	2.02	2.51	2.26	4.86	1.14	2.16
1.45	1.95	2.41	2.18	5.04	1.04	2.36
3.16	1.77	2.09	1.93	5.70	0.75	3.27

When the Metal Rubber components were installed with pre-compression, the bearing stiffness became larger. Use pre-strain to quantify the pre-compression in radial direction. While the radial pre-strain was 0.6%, the radial stiffness was 4.86×10^7 N/m and the angular stiffness was 2.16×10^5 N·m/rad. As the radial pre-strain increased to 3.16%, the radial stiffness increased to 5.70×10^7 N/m and the angular stiffness increased to 3.27×10^5 N·m/rad, by 17.3% and 51.6% respectively. The varying trends of the radial stiffness and angular stiffness with the pre-strain are shown in Fig.10. It's obvious that both the radial stiffness and the angular stiffness exhibited nonlinear increasing trend with the increase of the pre-compression. On the other hand, the angular stiffness is more sensitive to the pre-compression.

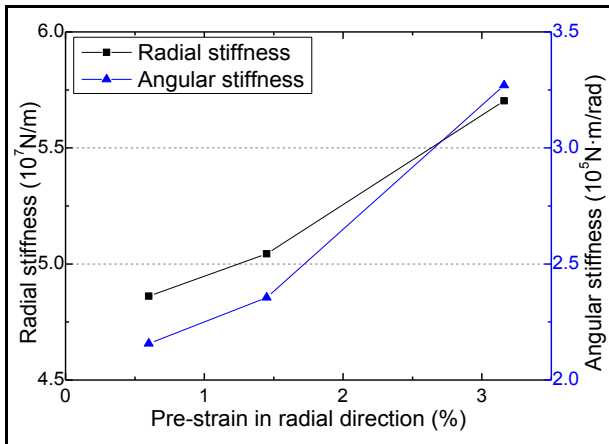


Fig.10 Support stiffness vs. pre-compression in radial direction

5 Conclusion

Through the simulation, the conclusions below are obtained:

(1) The stiffness of the the SC-MR support, including the radial stiffness and the angular stiffness, are mainly supplied by the squirrel

cage and the MR supplies minor parallel stiffness. The stiffness can be designed by controlling the parameters of the squirrel cage or the MR.

(2) The loading position has a great effect on both the radial stiffness and the angular stiffness. While the loading position moved from the left ring to the right one, the radial stiffness of the squirrel cage and the SC-MR support both varied by about 25%, and the angular stiffness varied by about 80%. The installation of the Metal Rubber has little effect on the varying amplitude of the radial stiffness, but contributes to an increase in the varying amplitude of the angular stiffness.

(3) The pre-strain of the MR has a significant effect on the compression mechanics of the SC-MR support. The radial stiffness and angular stiffness both exhibit nonlinear increasing trends with the radial prestrain. The angular stiffness is sensitive to the pre-compression. While the radial prestrain increased from 0.6% to 3.16%, the radial stiffness increased by 17.3% and the angular stiffness increased by 51.6%.

(4) The angular stiffness of the SC-MR support is more sensitive to either the loading position or the pre-compression. So during the designing, the angular stiffness should also be taken into account together with the radial stiffness.

References

- [1] Gu J, Ding K, Liu Q, et al. *Rotor Dynamics*. National Defence Industry Press, 1985.
- [2] Taylor D, Kumar B. Nonlinear Response of Short Squeeze Film Dampers. *Journal of Lubrication Technology*, Vol. 102, No.1, pp 51-58, 1980.
- [3] Holms R, Dogan M. Investigation of a Rotor Bearing Assembly Incorporating a Squeeze Film Damper

- Bearing. *Journal of mechanical engineering science*, Vol.24, No.3, pp 129-137, 1982.
- [4] Ma Y, Hong J, Zhao F. Theoretical Investigation of Vibration Attenuation Mechanism of an Adaptive Squeeze Film Damper. *Journal of Beijing University of Aeronautics and Astronautics*, Vol.30, No.1, pp 5-8, 2004.
- [5] Ma Y, Lu H, Zhu H, et al. Structural Design and Experiments of Elastic Ring-Metal Rubber Damper. *Acta Aeronautica et Astronautica Sinica*, Vol.34, No.6, pp 1301-1308, 2013.
- [6] Luis S, Thomas A, Kim T. Measurement of Structural Stiffness and Damping Coefficients in a Metal Mesh Foil Bearing. *Journal of engineering for gas turbines and power*, Vol.132, No.3, 2010.
- [7] Jiang H, Ao H, Xia Y, et al. Research on Manufacturing Technology and Application of Metal Rubber. *Modern Manufacturing Engineering*, Vol.8, pp 35-36, 2001.
- [8] Zhang D, Scarpa F, Ma Y, et al. Compression Mechanics of Nickel-based Superalloy Metal Rubber. *Materials Science & Engineering A*, Vol.580, pp 305-312, 2013.
- [9] Chegodayev D. *The Designing of Components Made of Metal Rubber*, Industry Publishing Company of National Defence, (Translated by Li Zhongge) , 2000.
- [10] Guo B, Zhu Z. Application of Metal Rubber Damper to the Rotor System. *Journal of Aerospace Power*, Vol.18, No.5, pp 662-668, 2003.
- [11] Al-Khateeb E, Vance J. Experimental evaluation of a metal mesh bearing damper in parallel with a structural support. *Proceedings of ASME*, Paper No.2001-GT-0247, 2001.
- [12] Al-Khateeb E. Design, Modeling and Experimental Investigation of Wire Mesh Vibration Dampers. *Ph.D. Thesis*, Texas A&M University, TX, USA, 2002.
- [13] Zhu B, Ma Y, Hong J. Theoretical Analysis on Stiffness and Damping Characteristics of Metal Rubber. *Journal of Beijing University of Aeronautics and Astronautics*, Vol.37, No.10, pp 1298-1302, 2011.
- [14] Zhang D, Scarpa F, Ma Y, et al. Dynamic mechanical behavior of nickel-based superalloy metal rubber. *Materials and Design*, Vol.56, pp 69-77, 2013.
- [15] Zarzour M. Experimental Evaluation of a Metal-Mesh Bearing Damper in a High Speed Test Rig. *M.S. thesis*, Department of Mechanical Engineering, Texas A&M University, TX, USA, 1999.
- [16] Zarzour M, Vance J. Experimental Evaluation of a Metal Mesh Bearing Damper. *Journal of engineering for gas turbines and power*, Vol.122, No.2, pp 326-329, 2000.
- [17] Ertas B, Al-Khateeb E, Vance J. Cryogenic temperature effects on metal mesh dampers and liquid hydrogen turbopump rotordynamics. *Proceedings of AIAA*, Paper No.AIAA-2002-4164, pp 7-10, 2002.
- [18] Ertas B, Al-Khateeb E, Vance J. Rotordynamic bearing dampers for cryogenic rocket engine turbopumps. *Journal of propulsion and power*, Vol.19, No.4, pp 674-682, 2003.
- [19] Choudhry V. Experimental evaluation of wire mesh for design as a bearing damper. *Doctoral dissertation*, Texas A&M University, TX, USA, 2004.
- [20] Lund J. Calculation of stiffness and damping properties of gas bearings. *Journal of Lubrication Technology*, Vol.90, No.4, pp 793-803, 1968.
- [21] Brommundt E. High-Order Sub-Harmonic Synchronization in a Rotor System with a Gear Coupling. *Technische Mechanik*, Vol.24, No.3-4, pp 242-253, 2004.

Contact Author Email Address

Mailto: zhx1011@yeah.net

Copyright Statement

The authors confirm that they, and/or their company or organization, hold copyright on all of the original material included in this paper. The authors also confirm that they have obtained permission, from the copyright holder of any third party material included in this paper, to publish it as part of their paper. The authors confirm that they give permission, or have obtained permission from the copyright holder of this paper, for the publication and distribution of this paper as part of the ICAS 2014 proceedings or as individual off-prints from the proceedings.